ICRF antenna coupling in ASDEX Upgrade 3D plasmas

G. Suárez López[1,2], R. Ochoukov[1], M. Willensdorfer[1], H. Zohm[1,2], D. Aguiam[3], V. Bobkov[1], M. Dunne[1], H. Faugel[1], H. Fünfgelder[1], J.-M. Noterdaeme[1,4], E. Strumberger[1], W. Suttrop[1], the ASDEX Upgrade Team,* and the EUROfusion MST1 Team.†

[1] *Max Planck Institute for Plasma physics, Garching b. Munchen, Germany*

[2] *Ludwig-Maximilians-University of Munich, Munich, Germany.*

[3] *Instituto de Plasmas e Fusao Nuclear, Universidade de Lisboa, Lisboa, Portugal*

[4] *Applied Physics Department, University of Ghent, Ghent, Belgium*

Introduction: Ion cyclotron range of frequencies (ICRF) heating is a widespread method for plasma heating in experimental fusion reactors. It relies on the excitation of the fast mode of a magnetized plasma at a frequency matching the cyclotron frequency of a given ionic species in the plasma core, such that resonant damping can occur. The fast wave, however, is evanescent from where it is excited due to the low-density conditions in the plasma edge, and the given antenna $k_{\parallel}$ spectrum. The cold plasma dispersion relation can be approximated as [6]:

$$n_{\perp}^2 = \frac{(R - n_{\parallel}^2)(L - n_{\parallel}^2)}{S - n_{\parallel}^2} \tag{1}$$

Where R, L and S are the elements of the cold plasma dielectric tensor and $n_{\parallel,\perp} = ck_{\parallel,\perp}/\omega$ is the parallel/perpendicular refractive index. The evanescent region is defined as the volume from the antenna to the R-cutoff where $R = n_{\parallel}^2$ such that $n_{\perp}^2 = 0$. The minimization of this volume is beneficial for the ICRF system, as it improves the accessibility of the fast wave to the core plasma, and thus relaxes the voltages in the feeding lines. Undesirably, plasma instabilities such as MHD modes and edge localized modes (ELMs) modify the edge density and thus change ICRF coupling [3] . A controlled way to study the effect of non-axisymmetric MHD modes on ICRF coupling is through the application of magnetic perturbations (MPs) from in-vessel saddle coils. At the same time, the effect of MPs themselves on ICRF coupling can be quantified in this manner [5]. In this paper, we describe a set of coupling experiments conducted on the ASDEX Upgrade tokamak in which MPs were applied on discharges with ICRF heating.

ASDEX Upgrade experiments: ICRF coupling can be influenced by MPs in two ways. On the one hand, the known pump-out effect tends to improve ICRF coupling as it produces a relaxation of the density profiles in the Scrape-Off Layer (SOL) [4]. On the other hand, the

*For a complete list of authors, see A. Kallenbach et al, Nucl Fus 57 (2017) 102015

†For a complete list of authors, see H. Meyer et al, Nucl Fus 57 (2017) 102014

plasma response to the MPs results in field-aligned kink displacements that compress or expand the density profiles [7]. In this study, we focus on the last effect.

A set of four H-mode discharges plus a reference one were performed in order to study the effect of MPs on ICRF coupling. The plasma parameters were kept constant with $B_t = -2.5\,\mathrm{T}$, $I_p = 0.8\,\mathrm{MA}$, resulting in an edge safety factor $q_{95} \sim 5.3$, with central

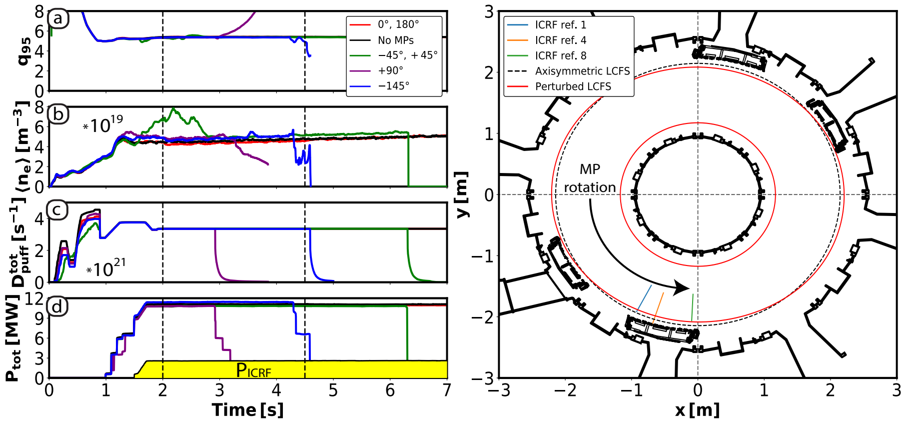

Figure 1: On the left, (a,b,c,d) time traces of the discharges: Safety factor at 95% poloidal flux q_{95}, line-averaged density $\langle n_e \rangle$, total deuterium puff D_{tot}^{puff} and total power P_{tot}. On the right, ICRF embedded reflectometry lines of sight and ICRF antennas. An axisymmetric and an exaggerated perturbed separatrix are shown.

electron density $n_e \sim 5 * 10^{19}\,\mathrm{m}^{-3}$. A total heating power of $P_{tot} \sim 12\,\mathrm{MW}$ was applied, out of which $P_{ICRF} \sim 2.7\,\mathrm{MW}$ was delivered simultaneously by 4 ICRF antennas in dipole phasing, resulting in a low pedestal top collisionality $\nu_e^* < 0.3$. The fraction of $P_{ICRF}/P_{tot} \sim 23\%$ was kept low as to reduce the impact of the changing coupling conditions on plasma global parameters. The rest of the heating power was supplied by NBI ($\sim 6.8\,\mathrm{MW}$) and ECRH ($\sim 2.5\,\mathrm{MW}$). The MPs were switched on at 2 seconds, during the flat top of the discharge and were supplied with $I_{coil} = 5\,\mathrm{kA} \times$ turns. Two differential phasings $\Delta\varphi_{UL}$ between the upper and lower row of coils were applied per discharge in n=2 configuration and rotated with a frequency of $\nu = 3\,\mathrm{Hz}$ for diagnostic purposes. The last two discharges ended in prompt disruption, so only one $\Delta\varphi_{UL}$ phase was acquired for them, resulting in a set with $\Delta\varphi_{UL} = \{-145^\circ, -45^\circ, 0^\circ, +45^\circ, +90^\circ, 180^\circ\}$. For the discharge with $\Delta\varphi_{UL} = \{-45^\circ, +45^\circ\}$ a tungsten event produced a density spike from 1.5-3s, hence this time slice is rejected in the analysis. ICRF coupling conditions were assessed through measurements of the loading resistance. A voltage probe in the voltage anti-node of the transmission lines provides V_{max} and a directional coupler behind the matching system provides $P_{coupled}$, such that:

$$R_L = \frac{2P_{coupled}Z_0^2}{{V_{max}}^2} \tag{2}$$

Where Z_0 is the characteristic impedance of the line. The non-axisymmetric density profile in front of one of the three-strap antennas was obtained with embedded reflectometry [1] with three active channels, labeled as {1,4,8} in **figure 1**. The R-cutoff position is obtained from **eq. 1** with the assumption of a H-D mixture of 5%-95% in the plasma, and using the CLISTE axisymmetric magnetic induction field calculation. This way, the total tokamak field is included in the analysis, although a small error is made in considering a pure axisymmetric field. For the three-strap antennas, a value of $k_{\parallel} = 11\,m^{-1}$ is usually representative for dipole phasing, as the power balance between the central and outer straps was kept at 2:1 [2], however, the R-cutoff was positioned beyond the density measurements for this $k_{\parallel}$, thus two values of $k_{\parallel} = 6\,m^{-1}$ (for Ref. 8) and $8\,m^{-1}$ (for Ref.1 and Ref.4), the latter being the main parallel wavenumber for the two-strap antennas spectrum, are used to illustrate the cutoff behavior instead. Since the reflectometer uses X-mode, the maximum resolvable depth differs among channels depending on their radial location inside the vessel. Density and coupling measurements are presented in **figure 2** for the $\Delta\varphi_{UL} = \{0°, 180°\}$ discharge. All considered time traces were analyzed with ELM-filtered data. The density profiles are plotted along their line of sight distance d_{LOS}.

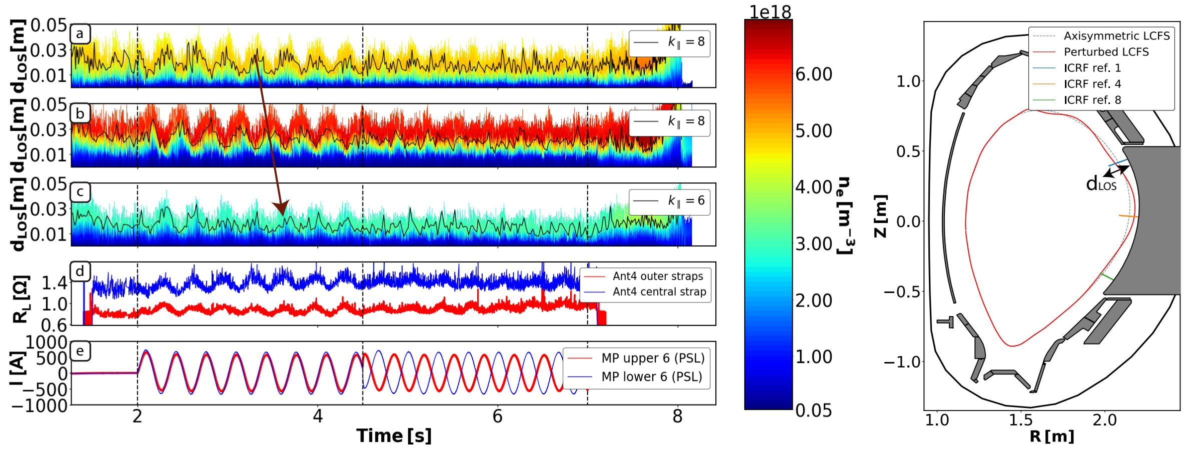

Figure 2: On the left, (a,b,c) density measurements at the different reflectometer channels Ref1, Ref4, Ref8 plotted along lines of sight, (d) Loading resistance measured at the feeders of the three-strap antenna, (e) applied currents to the MPs corrected for the PSL attenuation. The arrow marks the direction of rotation of the kink displacement along the antenna. On the right plot, the poloidal cross section of ASDEX Upgrade with reflectometer channels.

A clear density oscillation is observed in front of the ICRF antenna when the MPs are rotated. This corresponds to excited stable kink modes being rotated in front of the antenna. The R-cutoff position oscillates with the density profile, and the amplitude of the oscillation directly depends on the $k_{\parallel}$ value, with larger oscillations the larger $k_{\parallel}$ is. Coherent coupling oscillations are registered as measured in the two feeding lines of the same antenna. It is worth noting that when the MPs change from in-phase ($\Delta\varphi_{UL} = 0°$) to out of phase ($\Delta\varphi_{UL} = 180°$), the plasma response changes, decreasing the displacements in front of the antenna and thus the coupling oscillations. It is well-known that the plasma kink displacement varies as a function of the applied poloidal spectra from the MPs, $\Delta\varphi_{UL}$. By performing a least square sinusoidal fit to the loading resistances for every one of the applied $\Delta\varphi_{UL}$ phasings, the coupling amplitude variation can be obtained. This is displayed in **figure 3**, where ΔR_L^{feed} is the amplitude of the sinusoidal fit and $\langle R_L \rangle$ is the loading resistance time average of the considered window. The noise level of the fit is calculated by performing the same sinusoidal fit to the loading resistances for the discharge with no MPs, and then taking the average. The error bars represent the uncertainty of the fit alone. It is to be noted that induced currents on the passive stabilization loop (PSL) due to the MP rotation, lag and attenuate the strength of the MP field with respect to its DC value. Therefore, the resultant field is slightly out of phase with respect to the applied coil currents.

A clear dependence of the loading resistance oscillation amplitude on the applied $\Delta\varphi_{UL}$ is observed well above the noise level. This corroborates the picture of the coupling change being directly correlated to the plasma kink displacements. A maximum amplitude of 10% is reached, with a similar behavior between the two-strap antennas and the three-strap antennas. Nevertheless, larger coupling changes are expected, well correlated with larger plasma displacements, if the MP field attenuation becomes smaller, for instance, with slower MP rotation frequencies or larger coil currents.

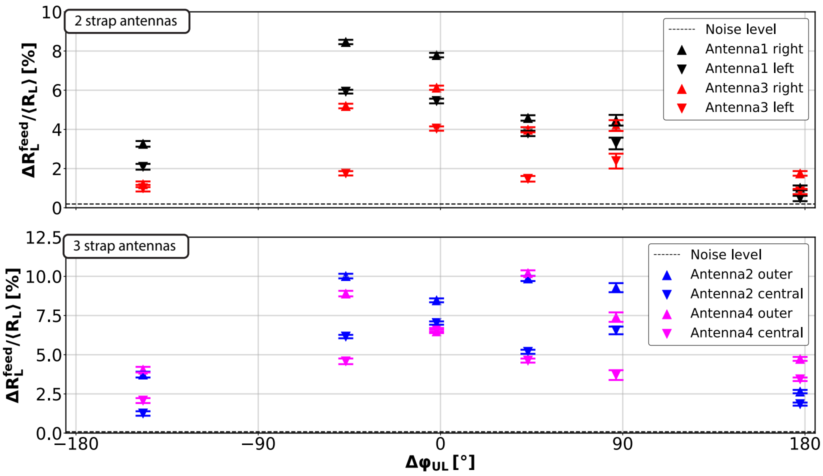

Figure 3: Loading resistance percentage change for the (upper) 2-strap antennas and (lower) 3-strap antennas. Left and right straps from the 2-strap antennas, as seen from the antenna reference frame towards the plasma. Outer straps in each three-strap antenna are connected to the same feeder.

Conclusions: The influence of MP-induced plasma displacements on ICRF coupling has been characterized for H-mode discharges in ASDEX Upgrade. Density variations due to the excited kink modes produce accompanying displacements of the fast wave R-cutoff, which in turn causes antenna coupling changes. Rotation of the kink modes in front of the antennas produces periodic coupling variations up to 10%, coherent with the MP field rotation.

Acknowledgments: This work has been carried out within the framework of the EUROfusion Consortium and has received funding from the Euratom research and training programme 2014-2018 under grant agreement No 633053. The views and opinions expressed herein do not necessarily reflect those of the European Commission

References

[1] D. E. Aguiam et al. In: *Review of Scientific Instruments* 87.11 (2016).

[2] V. Bobkov et al. In: *Nuclear Fusion* 56.8 (2016).

[3] V. Bobkov et al. In: *Nuclear Fusion* 46.7 (2006).

[4] V. Bobkov et al. In: *AIP Conference Proceedings* 1580.2014 (2014).

[5] G. S. López et al. In: *EPJ Web of Conferences* 157 (2017).

[6] T.H.Stix. AIP, New York, 1992.

[7] M. Willensdorfer et al. In: *Nuclear Fusion* 57.11 (2017).